

# Photo Voltaic cell Integrated DVR for Power Quality Improvement

G.Saritha  
M-tech Student

Department of Electrical & Electronics Engineering,  
Malla Reddy Engineering College (Autonomous)  
[golisaritha85@gmail.com](mailto:golisaritha85@gmail.com)

Ms.J.Srineswari  
Assistant Professor

Department of Electrical & Electronics Engineering,  
Malla Reddy Engineering College (Autonomous)  
[srineswari.jarapala@gmail.com](mailto:srineswari.jarapala@gmail.com)

**Abstract:** "Grid integration of distributed energy resources (DERs) is increasing rapidly. Integration of various types of energy storage technologies like batteries, ultra capacitors (UCAPs), superconducting magnets and flywheels to support intermittent DERs, such as solar and wind, in order to improve their reliability is becoming necessary. Of all the energy storage technologies UCAPs have low energy density, high power density and fast charge/discharge characteristics. They also have more charge/discharge cycles and higher terminal voltage per module when compared to batteries. All these characteristics make UCAPs ideal choice for providing support to events on the distribution grid which require high power for short spans of time. UCAPs have traditionally been limited to regenerative braking and wind power smoothing applications.

The major contribution of this dissertation is in integrating UCAPs for a broader range of applications like active/reactive power support, renewable intermittency smoothing, voltage sag/swell compensation and power quality conditioning to the distribution grid. Renewable intermittency smoothing is an application which requires bi-directional transfer of power from the grid to the UCAPs and vice-versa by charging and discharging the UCAPs. This application requires high active power support in the 10s-3min time scale which can be achieved by integrating UCAPs through a shunt active power filter (APF) which can also be used to provide active/reactive power support. Temporary voltage sag/swell compensation is another application which requires high active power support in the 3s-1min time scale which can be provided integrating UCAPs into the grid through series dynamic voltage restorer (DVR). All the above functionalities can also be provided by integrating the UCAPs into a power conditioner topology." The proposed concept is implemented to PV Applications by using Mat lab/simulink Software.

**Index Terms**—DC-DC converter,  $d-q$  control, DSP, dynamic voltage restorer (DVR), energy storage integration, phase locked loop (PLL), sag/swell, Ultra capacitor (UCAP).

## I. INTRODUCTION

Today photovoltaic (PV) power systems are turn into more and more famous, with the growth of energy

requirement and the matter of ecosystem pollution around the planet. Four dissimilar system configurations are extensively progressed in grid-connected PV power applications: the module integrated inverter system, the centralized inverter system, the multi-string inverter system and the string inverter system. Chiefly three kinds of inverter systems except the centralized inverter system can be involved as small-scale distributed generation (DG) systems, such as residential power applications. The most chief model limitation of the PV DG system is to attain a high voltage gain. For a characteristic PV module Power Quality conundrums cover a extensive range of disruptions such as voltage swells/sags, harmonics distortion, flicker, interruption and impulse transients [1]. Voltage sags can exists at any moment of time, with amplitudes extending from 10 – 90% and a duration lasting for half a cycle to one minute [3]. Voltage swell, on the other hand, is explained as a swell is explained as a rise in current or rms voltage at the power frequency for durations from 0.5 cycles to 1 minute. Characteristic magnitudes are between 1.1 and 1.8 pu. Swell magnitude is also explained by its persisting voltage, in this case, always greater than 1.0. [2, 3, 4].

Stability limits explain the extreme electrical power to be transferred without causing devastation to electric appliances and transmission lines. In principle, regulations on power transmission can always be diminished by the addition of new generation and transmission facilities. Alternatively, FACTS controllers can allow the same goals to be met with no chief adaptations to system layout. The potential benefits brought about by FACTS controllers include reduction of operation and transmission investment cost, increased system security and reliability, increased power transfer capabilities, and an overall enhancement of the quality of the electric energy delivered to customers Voltage swells are not much significant as voltage sags because they are less frequent in distribution systems. Voltage swell and sag can effects sensitive appliances (such as found in chemical plants or semiconductor) to shut down or fail as

well as create a abundant current unbalance that could trip breakers or blow fuses. These results can be very costly for the customer, ranging from minor quality alterations to production downtime and apparatus damage [5-7].

Various types of rechargeable energy storage technologies based on superconducting magnets (SMES), flywheels (FESS), batteries (BESS), and ultra-capacitors (UCAPs) are compared in [10] for integration into advanced power applications such as DVR. Efforts have been made to integrate energy storage into the DVR system, which will give the system active power capability that makes it independent of the grid during voltage disturbances. In [11], cascaded H-bridge-based DVR with a thyristor-controlled inductor is proposed to minimize the energy storage requirements. In [12], flywheel energy storage is integrated into the DVR system to improve its steady-state series and shunt compensation.

This paper introduces Dynamic Voltage Restorer and its operating principle. Then, a simple control based on Hysteresis voltage control method is used to compensate voltage swells/sags. At the end, MATLAB/SIMULINK model based simulated results were extant to certify the productiveness of the suggested control method of DVR.

Voltage sag is the most serious power quality conundrums faced by industrial customers. Voltage sag is familiar causes for malfunctioning in production plants. Voltage sag is short term shrinkage in voltage magnitude. According to IEEE standard 1159 voltage sag is “a decrease in RMS voltage between 10 to 90 % at a power frequency for durations from 0.5 cycles to 1 minute” [13].

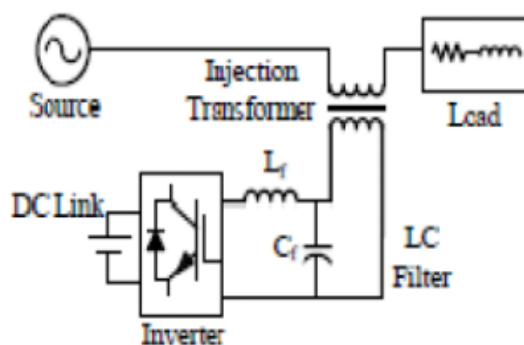


Fig.1. Basic Components of a DVR

During voltage sag, the DVR injects a voltage to restore the load supply voltages. The DVR needs a source for this energy. Two types of system are considered; one using stored energy to supply the delivered power as shown in Figure 1, and the other having no internal energy storage. There are a number of voltage swell/sag mitigating schemes available but the use of custom power

service is deliberated to the most productive scheme. This paper introduce basic concept of DVR (Dynamic Voltage Restore). DVR inject a compatible voltage magnitude with a compatible phase angle dynamically. Dynamic compensating signals are determine based on the difference between desired and actual values. Main components of DVR are voltage source converter, injecting transformer, passive filter, and energy storage device. The performance of DVR depends on the efficiency control technique of switching of voltage source inverter (VSI). In this paper Hysteresis Voltage control based simple control method is used to compensate voltage sag/swell.

## II. THREE-PHASE SERIES INVERTER

**A. Power Stage:** The one-line diagram of the system is shown in Fig. 2. The power stage is a three-phase voltage source inverter, which is connected in series to the grid and is responsible for compensating the voltage sags and swells; the model of the series DVR and its controller is shown in Fig. 3. The inverter system consists of an insulated gate bipolar transistor (IGBT) module, its gate-driver, LC filter, and an isolation transformer. The dc-link voltage  $V_{dc}$  is regulated at 260 V for optimum performance of the converter and the line–line voltage  $V_{ab}$  is 208 V; based on these, the modulation index  $m$  of the inverter is given by

$$m = \frac{2\sqrt{2}}{\sqrt{3}V_{dc} * n} V_{ab(rms)} \quad (1)$$

Where  $n$  is the turn's ratio of the isolation transformer. Substituting  $n$  as 2.5 in (1), the required modulation index is calculated as 0.52. Therefore, the output of the dc–dc converter should be regulated at 260 V for providing accurate voltage compensation. The objective of the integrated UCAPDVR system with active power capability is to compensate for temporary voltage sag (0.1–0.9 p.u.) and voltage swell (1.1–1.2 p.u.), which last from 3 s to 1 min.

**B. Controller Implementation** There are various methods to control the series inverter to provide dynamic voltage restoration and most of them rely on injecting a voltage in quadrature with advanced phase, so that reactive power is utilized in voltage restoration. Phase advanced voltage restoration techniques are complex in implementation, but the primary reason for using these techniques is

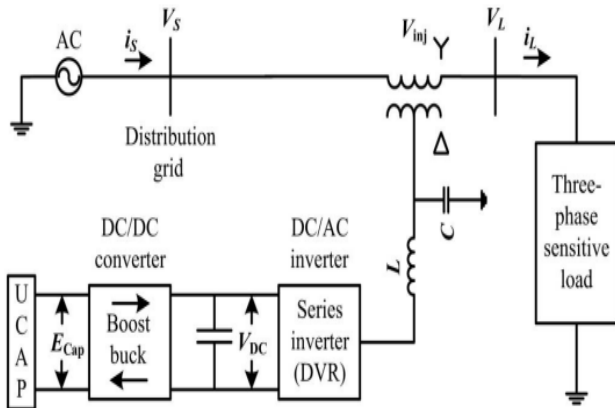


Fig. 2. One-line diagram of DVR with UCAP energy storage

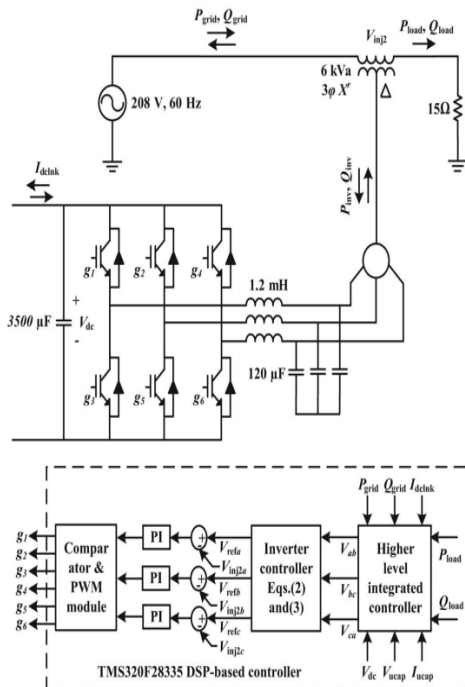


Fig. 3. Model of three-phase series inverter (DVR) and its controller with integrated higher order controller

to minimize the active power support and thereby the amount of energy storage requirement at the dc-link in order to minimize the cost of energy storage. However, the cost of energy storage has been declining and with the availability of active power support at the dc-link, complicated phase-advanced techniques can be avoided and voltages can be injected in-phase with the system voltage during a voltage sag or a swell event. The control method requires the use of a PLL to find the rotating angle. As discussed previously, the goal of this project is to use the active power capability of the UCAP-DVR system and compensate temporary voltage sags and

swells. The inverter controller implementation is based on injecting voltages in-phase with the supply-side line-neutral voltages. This requires PLL for estimating  $\theta$ , which has been implemented using the fictitious power method described. Based on the estimated  $\theta$  and the line-line source voltages,  $V_{ab}$ ,  $V_{bc}$ , and  $V_{ca}$  (which are available for this delta-sourced system) are transformed into the d-q domain and the line-neutral components of the source voltage  $V_{sa}$ ,  $V_{sb}$ , and  $V_{sc}$ , which are not available, can then be estimated using

$$\begin{bmatrix} V_{sa} \\ V_{sb} \\ V_{sc} \end{bmatrix} = \begin{bmatrix} 1 & 0 \\ -\frac{1}{2} & \frac{\sqrt{3}}{2} \\ -\frac{1}{2} & -\frac{\sqrt{3}}{2} \end{bmatrix} \begin{bmatrix} \cos(\theta - \frac{\pi}{6}) & \sin(\theta - \frac{\pi}{6}) \\ -\sin(\theta - \frac{\pi}{6}) & \cos(\theta - \frac{\pi}{6}) \end{bmatrix} \begin{bmatrix} \frac{V_d}{\sqrt{3}} \\ \frac{V_q}{\sqrt{3}} \end{bmatrix} \quad (2)$$

$$\begin{bmatrix} V_{refa} \\ V_{refb} \\ V_{refc} \end{bmatrix} = m * \begin{bmatrix} (\sin \theta - \frac{V_{sa}}{169.7}) \\ (\sin(\theta - \frac{2\pi}{3}) - \frac{V_{sb}}{169.7}) \\ (\sin(\theta + \frac{2\pi}{3}) - \frac{V_{sc}}{169.7}) \end{bmatrix} \quad (3)$$

$$P_{inv} = 3V_{inj2a(rms)} I_{La(rms)} \cos \varphi$$

$$Q_{inv} = 3V_{inj2a(rms)} I_{La(rms)} \sin \varphi \quad (4)$$

These voltages are normalized to unit sine waves using line-neutral system voltage of 120 V<sub>rms</sub> as reference and compared to unit sine waves in-phase with actual system voltages  $V_s$  from (3) to find the injected voltage references  $V_{ref}$  necessary to maintain a constant voltage at the load terminals, where  $m$  is 0.52 from (1). Therefore, whenever there is a voltage sag or swell on the source side, a corresponding voltage  $V_{inj2}$  is injected in-phase by the DVR and UCAP system to negate the effect and retain a constant voltage  $V_L$  at the load end. The actual active and reactive power supplied by the series inverter can be computed using (4) from the rms values of the injected voltage  $V_{inj2a}$  and load current  $I_{La}$ , and  $\varphi$  is the phase difference between the two waveforms.

### III. UCAP AND BIDIRECTIONAL DC-DC CONVERTER

**A. UCAP Bank:** The choice of the number of UCAPs necessary for providing grid support depends on the amount of support needed, terminal voltage of the UCAP, dc-link voltage, and distribution grid voltages. In this paper, the experimental setup consists of three 48 V, 165F UCAPs (BMOD0165P048) manufactured by Maxwell Technologies, which are connected in series. Therefore, the terminal voltage of the UCAP bank is 144 V and the dc-link voltage is programmed to 260 V. This would give the dc-dc converter a practical operating duty ratio of 0.44-0.72 in the boost mode while the UCAP is discharging and 0.27-0.55 in the buck mode while the UCAP is charging from the grid through the dc-link and the dc-dc converter. It is practical and cost-effective to

use three modules in the UCAP bank. Assuming that the UCAP bank can be discharged to 50% of its initial voltage ( $V_{uc,ini}$ ) to final voltage ( $V_{uc,fin}$ ) from 144 to 72 V, which translates to depth of discharge of 75%, the energy in the UCAP bank available for discharge is given by

$$E_{UCAP} = \frac{1}{2} * C * \frac{(V_{uc,ini}^2 - V_{uc,fin}^2)}{60} W - \text{min}$$

$$E_{UCAP} = 1/2 * 165/3 * (144^2 - 72^2) / 60$$

$$= 7128 W - \text{min.} \quad (5)$$

**B. Bidirectional DC-DC Converter and Controller:** A UCAP cannot be directly connected to the dc-link of the inverter like a battery, as the voltage profile of the UCAP varies as it discharges energy. Therefore, there is a need to integrate the UCAP system through a bidirectional dc-dc converter, which maintains a stiff dc-link voltage, as the UCAP voltage decreases while discharging and increases while charging. The model of the bidirectional dc-dc converter and its controller are shown in Fig. 4, where the input consists of three UCAPs connected in series and the output consists of a nominal load of 213.5  $\Omega$  to prevent operation at no-load, and the output is connected to the dc-link of the inverter. The amount of active power support required by the grid during a voltage sag event is dependent on the depth and duration of the voltage sag, and the dc-dc converter should be able to withstand this power during the discharge mode. The dc-dc converter should also be able

to operate in bidirectional mode to be able to charge or absorb additional power from the grid during voltage swell event. In this paper, the bidirectional dc-dc converter acts as a boost converter while discharging power from the UCAP and acts as a buck converter while charging the UCAP from the grid. A bidirectional dc-dc converter is required as an interface between the UCAP and the dc-link since the UCAP voltage varies with the amount of energy discharged while the dc-link voltage has to be stiff. Therefore, the bidirectional dc-dc converter is designed to operate in boost mode when the UCAP bank voltage is between 72 and 144 V and the output voltage is regulated at 260 V. When the UCAP bank voltage is below 72 V, the bidirectional dc-dc converter is operated in buck mode and draws energy from the grid to charge the UCAPs and the output voltage is again regulated at 260 V.

Average current mode control, which is widely explored in literature, is used to regulate the output voltage of the bidirectional dc-dc converter in both buck and boost modes while charging and discharging the UCAP bank. This method tends to be more stable when compared to other methods such as voltage mode control and peak current mode control. Average current mode controller is shown in Fig. 4, where the dc-link and actual output voltage  $V_{out}$  is compared with the reference voltage  $V_{ref}$  and the error is passed through the voltage compensator  $C_1(s)$ , which generates the average reference current  $I_{uref}$ . When the inverter is discharging power into the grid during voltage sag event, the dc-link voltage  $V_{out}$  tends to go below the reference  $V_{ref}$  and the error is positive;  $I_{uref}$  is positive and the dc-dc converter operates in boost mode. When the inverter is absorbing power from the grid during voltage swell event or charging the UCAP,  $V_{out}$  tends to increase above the reference  $V_{ref}$  and the error is negative;  $I_{uref}$  is negative and the dc-dc converter operates in buck mode. Therefore, the sign of the error between  $V_{out}$  and  $V_{ref}$  determines the sign of  $I_{uref}$  and thereby the direction of operation of the bidirectional dc-dc converter. The reference current  $I_{uref}$  is then compared to the actual UCAP current (which is also the inductor current)  $I_{uc}$  and the error is then passed through the current compensator  $C_2(s)$ . The compensator transfer functions, which provide a stable response, are given by

$$C_1(s) = 1.67 + \frac{23.81}{s} \quad (6)$$

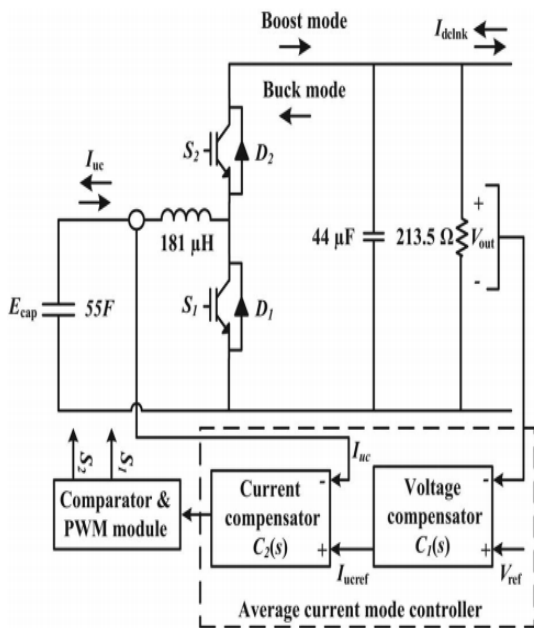


Fig. 4. Model of the bidirectional dc-dc converter and its controller

$$C_2(s) = 3.15 + \frac{1000}{s} \quad (7)$$

#### IV. PHOTOVOLTAIC SYSTEM

A Photovoltaic (PV) system directly converts solar energy into electrical energy. The basic device of a PV system is the PV cell. Cells may be grouped to form arrays. The voltage and current available at the terminals of a PV device may directly feed small loads such as lighting systems and DC motors or connect to a grid by using proper energy conversion devices this photovoltaic system consists of three main parts which are PV module, balance of system and load. The major balance of system components in this systems are charger, battery and inverter.

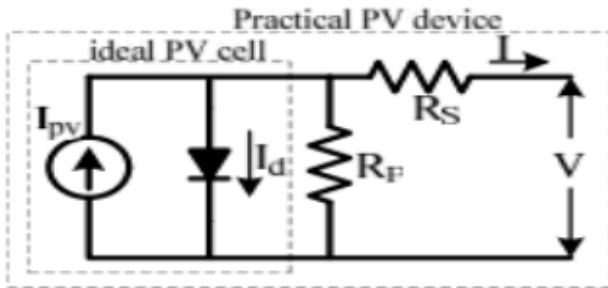


Fig.5. Practical PV device

A photovoltaic cell is basically a semiconductor diode whose p-n junction is exposed to light. Photovoltaic cells are made of several types of semiconductors using different manufacturing processes. The incidence of light on the cell generates charge carriers that originate an electric current if the cell is short circuited

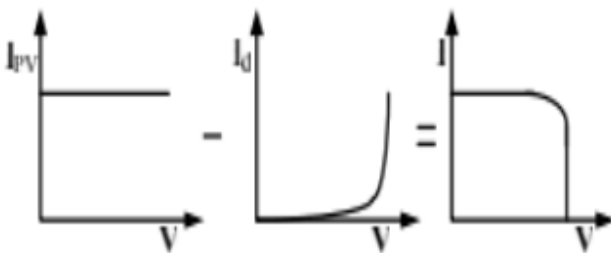


Fig.6. Characteristics I-V curve of the PV cell.

The equivalent circuit of PV cell is shown in the fig.5. In the above figure the PV cell is represented by a current source in parallel with diode. Rs and Rp represent series and parallel resistance respectively. The output current and voltage from PV cell are represented by I and V. The I-V characteristics of PV cell are shown in fig.6. The net cell current I is composed of the light generated current IPV and the diode current ID.

#### V. MATLAB/SIMULATION RESULTS

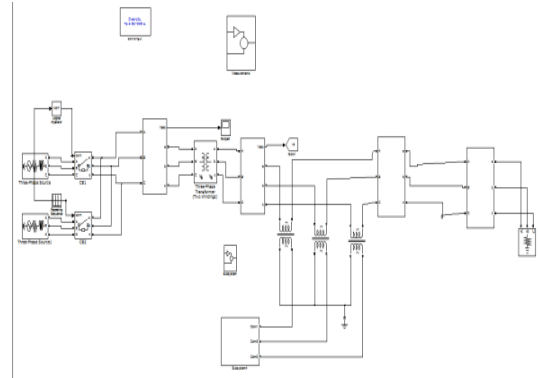


Fig 7 Matlab/simulation conventional method of sag generation

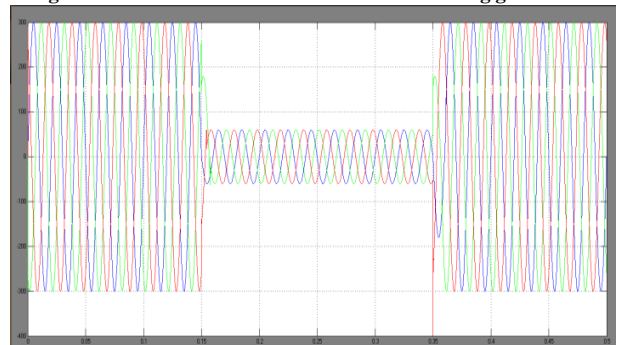


Fig 8 Source voltages  $V_{sab}$  (blue),  $V_{sbc}$  (red), and  $V_{sca}$  (green) during sag

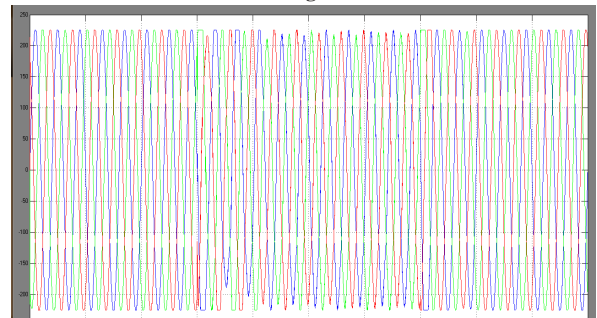


Fig 9 Load voltages  $V_{Lab}$  (blue),  $V_{Lbc}$  (red), and  $V_{Lca}$  (green) during sag.

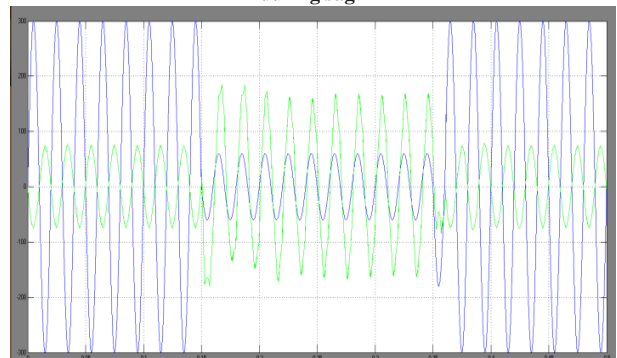
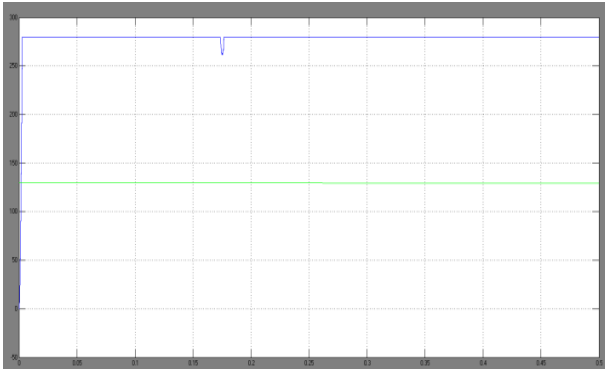
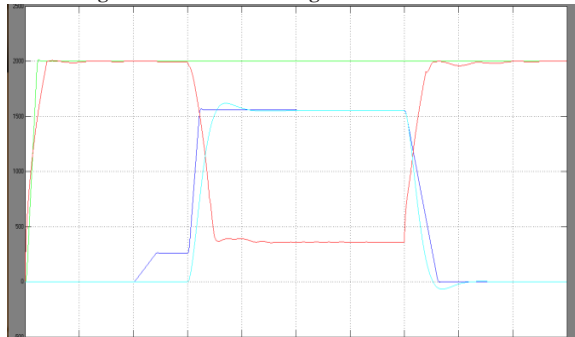


Fig 10  $V_{inj2a}$  (green) and  $V_{sab}$  (blue) waveforms during sag.



**Fig 11** Currents and voltages of dc-dc converter



**fig 12** Active power of grid, load, and inverter during voltage sag..

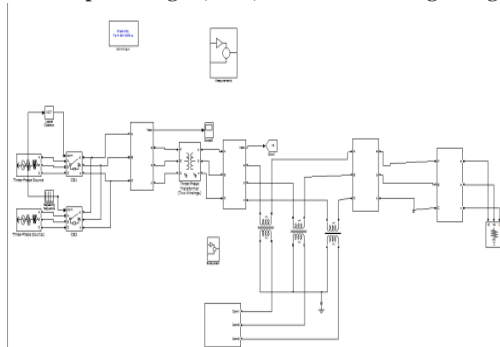


**Fig 13** Matlab/simulation conventional method of swell generation

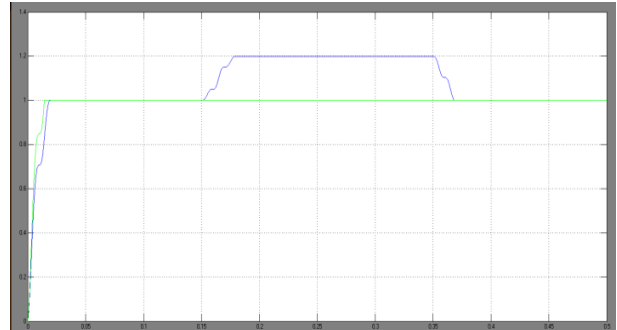


**Fig 14** Source and load rms voltages  $V_{rms}$  and  $V_{Lrms}$  during swell

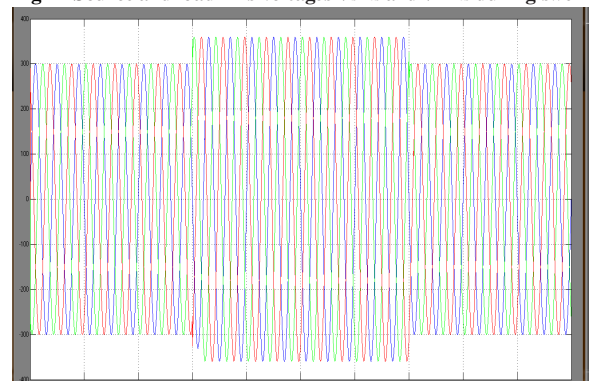


**Fig 15** Source voltages  $V_{sab}$  (blue),  $V_{sbc}$  (red), and  $V_{sa}$  (green) during swell

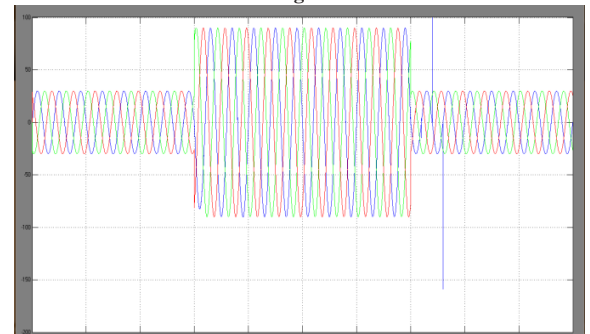


**Fig 16** Load voltages  $V_{Lab}$  (blue),  $V_{Lbc}$  (red), and  $V_{Lca}$  (green) during swell

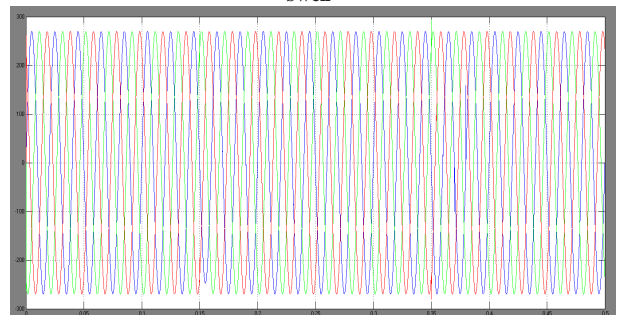


**Fig 17** Injected voltages  $V_{inj2a}$  (blue),  $V_{inj2b}$  (red),  $V_{inj2c}$  (green) during swell

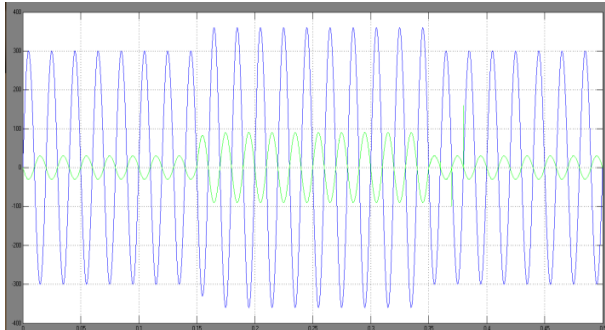


Fig 18  $V_{inj2a}$  (green) and  $V_{sab}$  (blue) waveforms during swell

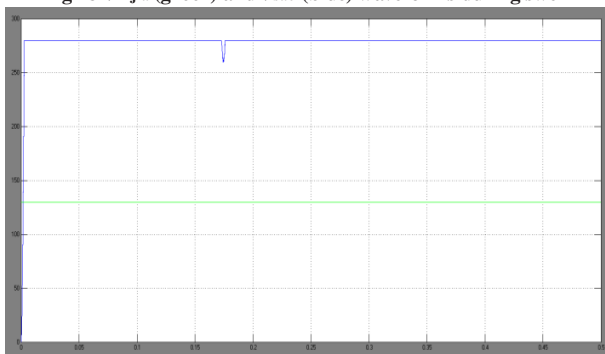


Fig 19 Currents and voltages of dc-dc converter during swell.

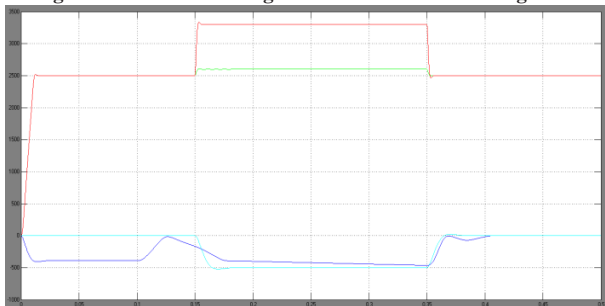


Fig 20 Active and reactive power of grid, load, and inverter during a voltage swell.

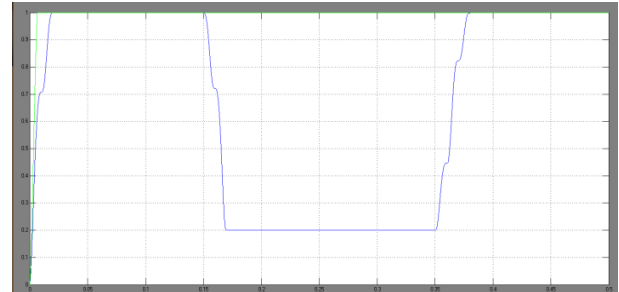


Fig 21 Source and load RMS voltages  $V_{srms}$  and  $V_{Lrms}$  during sag with PV cell

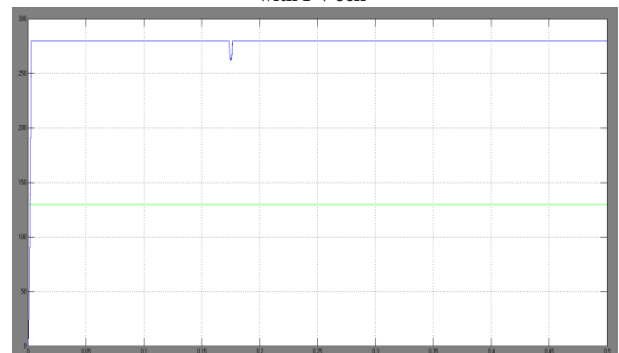


Fig 22 output voltage source of PV

## VI.CONCLUSION

In this result, the reputation of voltage in the distribution side was superior with the help of DVR, when the disturbance occurs in sensitive load feeder. Examination was carried out to various custom power devices, DVR having excellent damages for voltage disturbances. Simulation was carried out with PV interfaced multilevel converter based DVR employing sinusoidal PWM technique with MATLAB/SIMULINK software. Many paper worked on voltage improvement for sag or swell, but in the proposed model both are mitigated either required. To further boosts up the function of a DVR, we imply a few techniques It is observed that throughout fault condition the power factor at input side is maintained unity and we adding the PV source in input side. The total system output voltage is maintained constant throughout the fault condition.

## REFERENCES

- [1].Deepak Somayajula, Member, IEEE, and Mariesa L. Crow, Fellow, IEEE"An Integrated Dynamic Voltage Restorer-Ultracapacitor Design for Improving Power Quality of the Distribution Grid"IEEE Transactions On Sustainable Energy, Vol. 6, No. 2, April 2015
- [2] N. H. Woodley, L. Morgan, and A. Sundaram, "Experience with an inverter-based dynamic voltage restorer," IEEE Trans. Power Del., vol. 14, no. 3, pp. 1181–1186, Jul. 1999.
- [3] S. S. Choi, B. H. Li, and D. M. Vilathgamuwa, "Dynamic voltage restoration with minimum energy injection," IEEE Trans. Power Syst., vol. 15, no. 1, pp. 51–57, Feb. 2000.

- [4] D. M. Vilathgamuwa, A. A. D. R. Perera, and S. S. Choi, "Voltage sag compensation with energy optimized dynamic voltage restorer," *IEEE Trans. Power Del.*, vol. 18, no. 3, pp. 928–936, Jul. 2003.
- [5] Y. W. Li, D. M. Vilathgamuwa, F. Blaabjerg, and P. C. Loh "A robust control scheme for medium-voltage-level DVR implementation," *IEEE Trans. Ind. Electron.*, vol. 54, no. 4, pp. 2249–2261, Aug. 2007.
- [6] A. Ghosh and G. Ledwich, "Compensation of distribution system voltage using DVR," *IEEE Trans. Power Del.*, vol. 17, no. 4, pp. 1030–1036, Oct. 2002.
- [7] A. Elnady and M. M. A. Salama, "Mitigation of voltage disturbances using adaptive perceptron-based control algorithm," *IEEE Trans. Power Del.*, vol. 20, no. 1, pp. 309–318, Jan. 2005.
- [8] P. R. Sanchez, E. Acha, J. E. O. Calderon, V. Feliu, and A. G. Cerrada, "A versatile control scheme for a dynamic voltage restorer for power quality improvement," *IEEE Trans. Power Del.*, vol. 24, no. 1, pp. 277–284, Jan. 2009.
- [9] C. S. Lam, M. C. Wong, and Y. D. Han, "Voltage swell and overvoltage compensation with unidirectional power flow controlled dynamic voltage restorer," *IEEE Trans. Power Del.*, vol. 23, no. 4, pp. 2513–2521, Oct. 2008.
- [10] K. Sahay and B. Dwivedi, "Supercapacitor energy storage system for power quality improvement: An overview," *J. Elect. Syst.*, vol. 10, no. 10, pp. 1–8, 2009.
- [11] P. F. Ribeiro, B. K. Johnson, M. L. Crow, A. Arsoy, and Y. Liu, "Energy storage systems for advanced power applications," *Proc. IEEE*, vol. 89, no. 12, pp. 1744–1756, Dec. 2001.
- [12] H. K. Al-Hadidi, A. M. Gole, and D. A. Jacobson, "A novel configuration for a cascaded inverter-based dynamic voltage restorer with reduced energy storage requirements," *IEEE Trans. Power Del.*, vol. 23, no. 2, pp. 881–888, Apr. 2008.
- [13] R. S. Weissbach, G. G. Karady, and R. G. Farmer, "Dynamic voltage compensation on distribution feeders using flywheel energy storage," *IEEE Trans. Power Del.*, vol. 14, no. 2, pp. 465–471, Apr. 1999.